AIAA JOURNAL
Vol. 39, No. 4, April 2001

Effects of Reaction Mechanisms on Structure and Extinction of Partially Premixed Flames

H. S. Xue* and S. K. Aggarwal†
University of Illinois at Chicago, Chicago, Illinois 60607

The structure and extinction behavior of partially premixed flames in a counterflow configuration are investigated by using five different chemistry models. These include the C_1 and C_2 mechanisms of Peters and Rogg (Peters, N., and Rogg, B., *Reduced Kinetic Mechanisms for Applications in Combustion Systems*, Springer–Verlag, Berlin, 1993, pp. 8–12), a 12-step augmented reduced mechanism, and GRI-2.11 and GRI-3.0 mechanisms. Simulations focus on the comparison of these mechanisms in predicting the structure and extinction of methane–air partially premixed flames over a wide range of strain rates and equivalence ratios, including those corresponding to premixed and diffusion flames. Premixed flame speeds calculated using the C_2 and GRI-2.11 mechanisms are in good agreement with the experimental data, whereas those obtained using the C_1 mechanism show significant differences, especially for fuel-rich conditions. The predicted flammability limits ($0.5 < \phi < 1.4$) are found to be nearly identical for the three mechanisms. In addition, the diffusion flame structures computed using the three mechanisms are essentially the same, except for small differences in the peak temperature values. Results for partially premixed flames indicate that all five mechanisms qualitatively reproduce the double-flame structure associated with these flames. There are, however, notable quantitative differences between the predictions of C_1, C_2, and GRI-2.11 mechanisms. For low to moderate strain rates and high levels of air premixing ($\phi < 2.0$), the rich premixed reaction zone for the GRI-2.11 and GRI-3.0 mechanisms is located very close to the fuel nozzle. In addition, the physical separation between the two reactions zones for these mechanisms is significantly larger compared to that for C_1 and C_2 mechanisms. Important quantitative differences are also observed in the predictions of C_1 and C_2 mechanisms. Compared to the C_1 mechanism, the predictions using the C_2 mechanism indicate that 1) the methane consumption and heat release rates in the premixed zone are higher, 2) the flame structure exhibits higher sensitivity to the equivalence ratio, and 3) the two reaction zones merge at a lower equivalence ratio. The extinction strain rates for partially premixed flames are significantly higher using the C_2 and GRI-2.11 mechanisms compared to those using the C_1 mechanism. The effect of radiation heat transfer, computed using an optically thin model on the partially premixed flame structure, is relatively small. Also note that the premixed flame speed plays an important role in determining the stretch rate and, therefore, the structure of partially premixed flames.

Introduction

A PARTIALLY premixed flame is characterized by the presence of synergistically coupled multiple reaction zones. A double partially premixed flame can be obtained by mixing air in less than stoichiometric amounts in the fuel stream and supplying air in the other stream. Compared with the premixed and diffusion (nonpremixed) flames, a partially premixed flame is capable of achieving both high-energy supply and low pollutant emissions simultaneously. Therefore, it is important to understand the structure and extinction behavior of partially premixed flames.

Amongst various hydrocarbon fuels, the methane oxidation chemistry has been investigated most extensively, and several detailed mechanisms have been reported. Yang and Puri[1] used a detailed reaction mechanism involving 27 species and 224 elementary steps to examine NO_x formation in premixed flames established far from extinction. Williams and Li[2] employed a detailed mechanism containing 177 elementary reactions to investigate NO_x formation in partially premixed methane–air flames. Blevins and Gore[3] employed the GRI-2.11 mechanism[4] to investigate the flame structure and NO reactions of low-strain-rate partially premixed flames. In their study, a low strain rate was obtained in the large central spatial region of the counterflow by imposing a radial velocity gradient at the boundaries of the computational domain. The GRI-2.11 mechanism considers the chemistry of C_1 and C_2 species, and NO, which involves 279 reactions and 49 species. Peters and Rogg[5] proposed a detailed mechanism consisting of 112 reactions and involving C_1, C_2, and C_3 species. Seshadri and Peters,[6] Seshadri,[7] and Buipham et al.[8] employed reduced mechanisms to analyze the flame structure by using an asymptotic approach. A four-step methane–air mechanism was employed, and the overall flame structure was divided into a preheated zone, a reaction zone, and a postflame zone. Burning velocities and characteristic temperatures were obtained for both the fuel-lean and fuel-rich methane–air mixtures.

In this paper, we investigate the structure and extinction behavior of methane–air partially premixed flames in a counterflow configuration. A schematic of the counterflow flame that contains two reaction zones is shown in Fig. 1. Compared with Bunsen-type and jet flames, a counterflow flame offers many advantages for fundamental investigations. The flame is quite stable and can be treated as a one-dimensional problem. Because the flame can be characterized by a single strain rate, it greatly facilitates the investigation of detailed chemistry models, flow–chemistry interactions, and identification of the dominant reaction pathways. (Note that a commonly used definition of an effective strain rate is the maximum value of the oxidizer-side velocity gradient just before the flame.[9] The same definition is employed in the present study.) The wide and flat flame is also amenable to detailed experimental measurements.

The structure of a partially premixed methane–air flame in a counterflow configuration was first investigated by Yamaoka and Tsuji.[10–12] From detailed measurements, it was established that the flame structure is characterized by two separated reaction zones, a rich premixed zone on the fuel side and a nonpremixed zone on the air side, and that the interactions between these two zones are determined by the combined effect of strain rate a_s and equivalence ratio ϕ. In addition, it was shown that the rich flammability limit of methane–air mixtures can be extended by using partially premixed combustion, and various stable flame configurations can

Received 7 June 1999; presented as Paper 2000-0578 at the AIAA 38th Aerospace Sciences Meeting, Reno, NV, 11–13 January 2000; revision received 16 June 2000; accepted for publication 11 July 2000.

*Graduate Student, Department of Mechanical Engineering.
†Professor, Department of Mechanical Engineering. Associate Fellow AIAA.

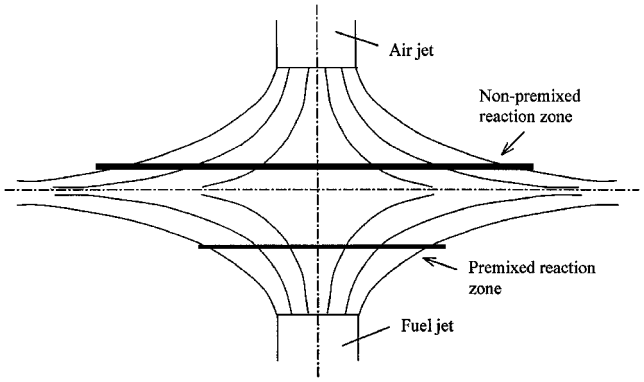

Fig. 1 Schematic of a partially premixed flame in a counterflow configuration.

be achieved by controlling the strain rate and equivalence ratio in the fuel stream. Subsequent studies[13–15] focused on the response of counterflow partially premixed flames to changes in a_s and ϕ. It was shown that as a_s is increased at a fixed ϕ (or ϕ is increased at a fixed a_s), the two reaction zones tend to merge. A further increase in a_s at a fixed ϕ then leads to flame extinction, whereas that in ϕ at a fixed a_s yields a typical diffusion flame structure. Whereas these studies provided fundamental information about the flame structure, the chemical and transport processes involved in the merging of the reaction zones were not investigated in detail. In addition, the role of premixed flame speed in determining the partially premixed flame structure was not examined.

The present study has two major objectives. One is to examine the detailed structure of partially premixed flames and the role of premixed flame speed in determining this structure. Because the flame comprises two spatially separated reaction zones, we also examine the interactions that determine their spatial separation and merging behavior. In this context, we also investigate the response of each reaction zone and, thereby, the flame response to the variations in strain rate and equivalence ratio. The effect of radiative heat transfer on the flame structure and extinction is also characterized.

The second objective is to examine the applicability of several detailed mechanisms for predicting the structure of methane–air partially premixed flames. The mechanisms include the C_1 and C_2 mechanisms of Peters and Rogg,[5] the GRI-Mech 2.11, the 12-step augmented reduced mechanism,[16] and the GRI-Mech 3.0. The C_1 mechanism involves only C_1 species and 52 elementary reactions, whereas the C_2 mechanism considers both C_1 and C_2 species and involves 81 elementary reactions. The 12-step augmented mechanism was reduced from GRI-Mech 1.2 and was validated by Sung et al.[16] for a wide range of combustion phenomena. The GRI-Mech 3.0 is the updated version of GRI-Mech 2.11.

The C_1 and C_2 mechanisms were employed recently by Shu et al.[17,18] to predict the partially premixed flame structure in a planar coflow configuration. Although some quantitative differences between their predictions were noted, the simulations using the two mechanisms were shown to reproduce the measured flame structure over a wide range of conditions. Because the C_1 mechanism has been known to be inadequate for fuel-rich flames, its satisfactory performance in the context of predicting coflow partially premixed flames is surprising and warrants further investigation. Another motivation for using the C_1, C_2, and GRI-2.11 mechanisms is due to a recent study of Katta and Roquemore,[19] which showed that the structure of coaxial jet diffusion flames computed by using these mechanisms was essentially the same. Because partially premixed flames involves both premixed and nonpremixed combustion, the present study examines the applicability of these mechanisms for premixed, nonpremixed, and partially premixed flames.

Numerical Model

The counterflow flame configuration employed in the present investigation is shown schematically in Fig. 1. Two coaxial nozzles are placed one above the other. Methane–air mixture flows from the lower nozzle and air from the upper nozzle. The separation distance between the two nozzles is 2 cm. Both the equivalence ratio and strain rate can be varied independently.

Simulations are performed using the Oppdif[20] and Chemkin[21,22] packages. Oppdif is a FORTRAN program that computes the flame and the flowfield in a counterflow configuration. The two-dimensional axisymmetric flowfield is transformed to a one-dimensional problem by employing a similarity transformation. When the assumptions are used that radial velocity varies linearly with radial distance, and gas properties vary only with axial distance, the dependent variables become functions of the axial direction only. Oppdif solves for the temperature, species mass fractions, axial and radial velocity components, and radial pressure gradient, which is an eigenvalue in the problem. The formulation results in a two-point boundary value problem after boundary conditions are specified at two nozzle exits.

The Chemkin package uses the kinetic mechanism as input and evaluates the chemical reaction rates as well as the thermodynamic and transport properties. The structure of partially premixed flames is analyzed by varying the fuel stream equivalence ratio ϕ and the aerodynamic strain rate a_s. The effects of C_1, C_2, and GRI-2.11 mechanisms on the computed flame structure and extinction behavior are then examined. In addition, a 12-step reduced mechanism and the GRI-3.0 mechanism are examined in the context of predicting the partially premixed flame structure.

Results and Discussion

Premixed Flame Speeds Computed with Different Reaction Mechanisms

The flame speed of methane–air mixture as a function of ϕ was computed by using the Chemkin[21,22] premixed flame package. The calculations were performed employing the C_1, C_2, and GRI-2.11 mechanisms. In Fig. 2, we plot the computed premixed flame speeds S_L vs ϕ for the three mechanisms and compare them with the experimental data reported by Vagelopoulos et al.[23] The predictions using the C_2 and GRI-2.11 mechanisms show good agreement with the measurements, except for some differences at fuel-lean conditions, whereas those using the C_1 mechanism exhibit significant differences at fuel-rich conditions. Not only does this mechanism underpredict the premixed flame speed, especially for $\phi > 0.7$, it also underpredicts the equivalence ratio corresponding to the maximum flame speed. The flammability limits predicted by the three mechanisms are $0.5 < \phi < 1.4$, whereas the experimental flammability limits are $0.5 < \phi < 1.5$.

Effect of Premixed Flame Speed on the Partially Premixed Flame Structure

The Oppdif package along with the C_2 mechanism is employed to compute the partially premixed flame structure in a counterflow configuration. The objective is to examine the role of premixed flame speed in determining the partially premixed flame structure. The values of GRAD and CURV, which control the grid size and distribution in Oppdif, are taken as 0.1. The grid independence was

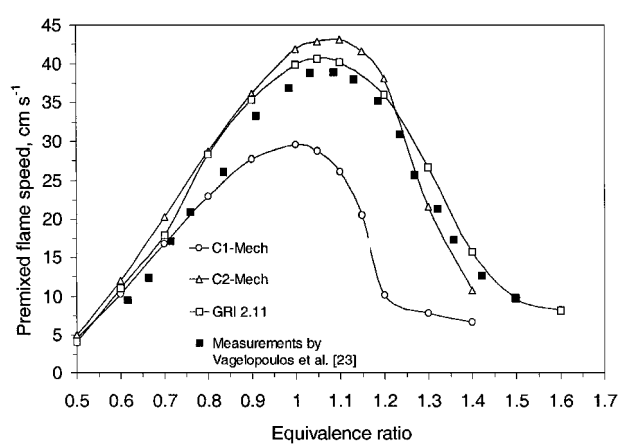

Fig. 2 Comparison of the premixed flame speed calculated by using C_1, C_2, and GRI-2.11 mechanisms with the experimental data reported by Vagelopoulos et al.[23]

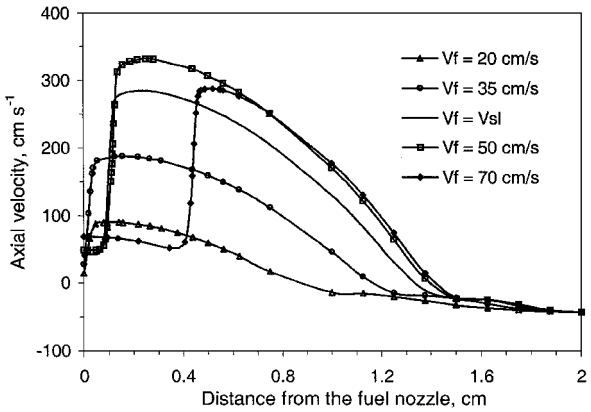

Fig. 3a Axial velocity profiles for different fuel stream velocities obtained by using the C_2 mechanism; $\phi = 1.1$, and airstream velocity is 43.12 cm/s.

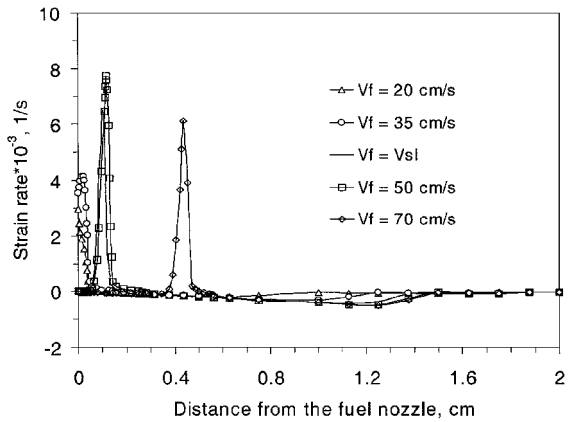

Fig. 3b Strain rate profiles for different fuel stream velocities.

examined by increasing the values of GRAD and CURV by a factor of 5. The difference in the computed flame structure for the two grids was negligible.

Figure 3a shows the axial velocity profiles in the region near the fuel nozzle exit for different fuel stream velocities. The airstream velocity is held constant at 43.12 cm/s and $\phi = 1.1$, which is within the flammability limit of methane–air mixtures. The flame speed obtained by using the C_2 mechanism for this case is $S_L = 43.12$ cm/s. When the fuel jet exit velocity V_f is less than S_L, the axial velocity increases continuously until it reaches the peak value. For $V_f = S_L$ and 50 cm/s, the axial velocity profile remains flat and then rises sharply as x approaches the reaction zone. For $V_f = 70$ cm/s, the axial velocity first decreases to about 50 cm/s and then increases abruptly near the flame.

The fuel side axial velocity gradients for various values of V_f are plotted in Fig. 3b. For $V_f < S_L$, the velocity gradient is quite high near the nozzle exit implying that the fuel stream accelerates there. However, for $V_f > S_L$, the fuel mixture has to decelerate to a velocity that corresponds to the premixed flame speed. This results in a negative velocity gradient near the nozzle exit. For $V_f = S_L$, the velocity gradient is very low. As indicated by Tanoff and Smooke,[13] the maximum fuel-side velocity gradient is an extremely sensitive indicator of the flame character for counterflow partially premixed flames. An important observation here is that the premixed reaction zone of the partially premixed flames has an apparent propagation velocity, which can be approximately determined as the lowest value of the axial velocity just upstream of the premixed reaction zone. Note that the propagation velocity is not the same for all of the mentioned cases because the detailed structure of the partially premixed flame varies with V_f. Nevertheless, it can be argued that the premixed flame speed plays an important role in determining the detailed structure of a partially premixed flame because it affects the stretch rate. Moreover, because the C_2 mechanism predicts the laminar flame speeds more accurately than the C_1 mechanism, it is inferred that the partially premixed flame structure is predicted more accurately using the C_2 mechanism than that using the C_1 mechanism.

Effect of Reaction Mechanisms on the Partially Premixed Flame Structure

To investigate the effects of reaction mechanisms on the structure of partially premixed flames, simulations are performed for two levels of air premixing, $\phi = 1.5$ and 3.0, and for a moderate strain rate of 7.5 s^{-1}. This strain rate is obtained by setting the exit velocities of the fuel and oxidizer streams at 10 cm s^{-1}. The plug flow boundary conditions are employed in the computational model.

Figure 4 shows the computed flame structure in terms of temperature profiles, obtained by using the C_1, C_2, and GRI-2.11 mechanisms. The corresponding species mole fraction profiles are presented in Fig. 5. These profiles indicate significant differences in the structure of partially premixed flames predicted by the three mechanisms. In contrast, the temperature profiles for the corresponding diffusion flame at the same strain rate indicate an almost identical flame structure for the three mechanisms (cf. Fig. 6). The latter result is consistent with that reported by Katta and Roquemore[19] concerning the effects of different chemistry models on the computed diffusion flame structure. The C_1 mechanism yields a slightly higher temperature compared to that obtained using the C_2 and GRI-2.11 mechanisms, which is due to the endothermic reactions associated with C_2 chemistry that is included in the latter two mechanisms. This result is also in accord with that reported by Katta and Roquemore.[19] An important implication is that the inclusion of C_2 chemistry affects the structure of the rich premixed reaction zone.

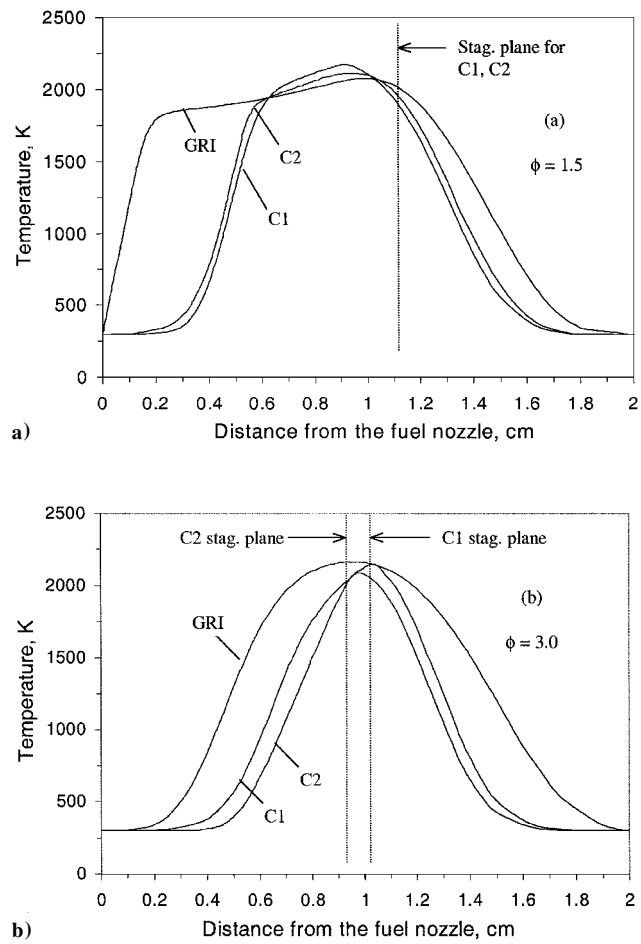

Fig. 4 Partially premixed flame structure in terms of temperature profiles obtained using C_1, C_2, and GRI-2.11 mechanisms with fuel and airstream velocities of 10 cm/s each and 7.5 s^{-1} strain rate for a) $\phi = 1.5$ and b) $\phi = 3.0$.

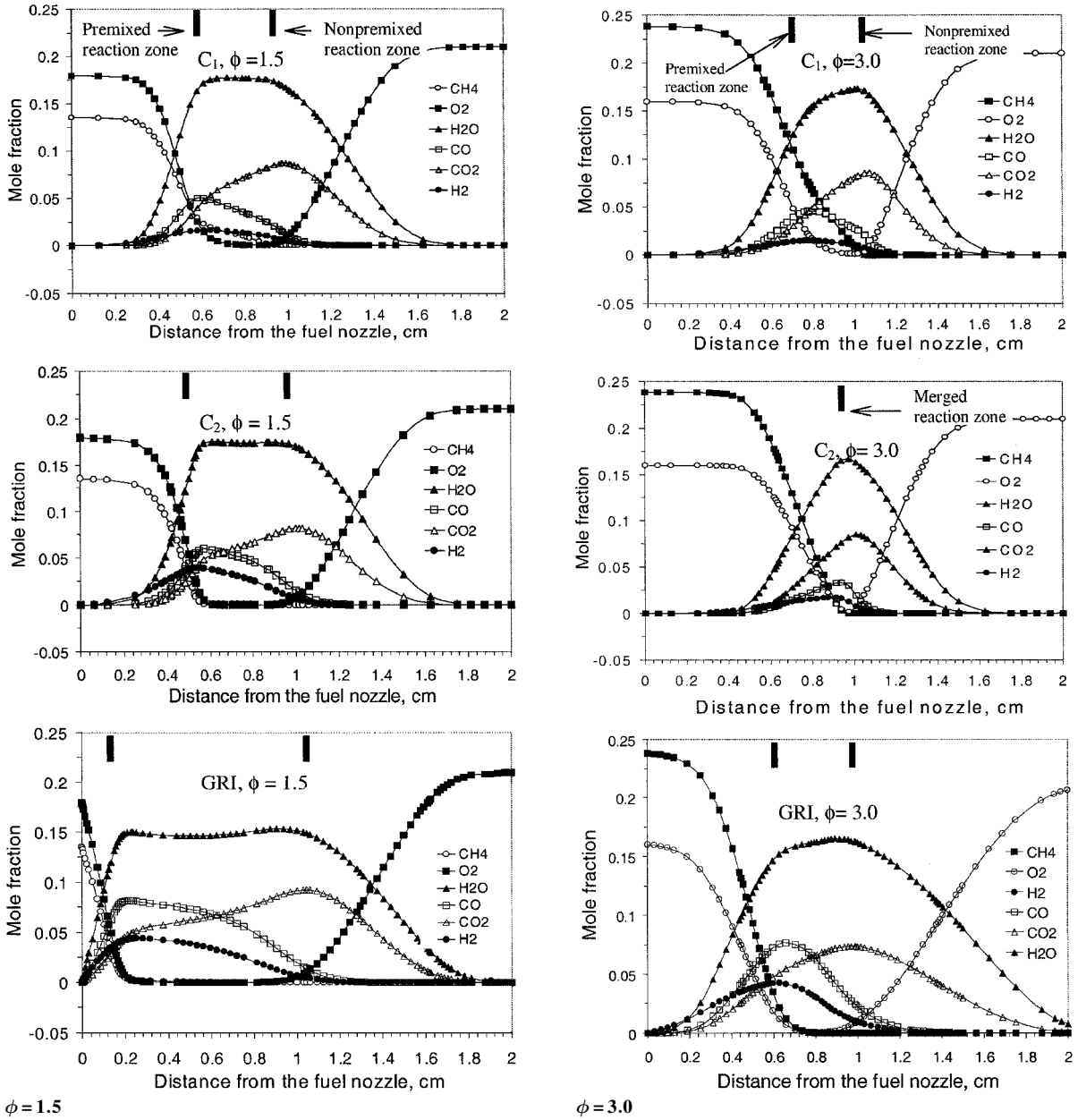

Fig. 5 Major species mole fraction profiles for the partially premixed flame computed using C_1, C_2, and GRI-2.11 mechanisms.

The scalar profiles in Figs. 4 and 5 indicate that all three mechanisms reproduce qualitatively the global structure of partially premixed flames obtained in laboratory experiments.[10–12] The global flame structure pertains to the existence of two reaction zones, namely, a rich premixed reaction zone on the fuel side and a nonpremixed reaction zone on the air side, and the synergistic interactions between them. The premixed zone is dominated by the fuel consumption chemistry, whereby CH_4 and O_2 react with H and OH radicals to produce CO and H_2, which then become the reactant or fuel species for the nonpremixed zone, where they are oxidized to form CO_2 and H_2O. The nonpremixed zone, being the zone of highest temperature, in turn provides the heat and radical species (such as H and OH) to the premixed zone. The nonpremixed zone chemistry is dominated by the H_2–O_2 reactions, CO oxidation, and the production of CO_2 and H_2O. This is clearly indicated by the peaks in CO and H_2 mole fractions in the premixed zone and the peak in CO_2 that occurs in the nonpremixed zone. The peak in H_2O occurs at a lower axial location compared to that in CO_2 because the H_2O formation rate is higher than that of CO_2.

Whereas all three mechanisms reproduce the double-flame structure associated with partially premixed flames, they also exhibit significant quantitative differences. In particular, the GRI-2.11 mechanism yields a flame structure that is markedly different from those obtained using the other two mechanisms. At $\phi = 1.5$, the rich premixed reaction zone for the GRI-2.11 mechanism is located very close to the fuel nozzle, causing significant heat loss to the nozzle. In addition, the global flame with this mechanism is significantly broader than that with the other two mechanisms (cf. Figs. 4 and 5). This is somewhat unexpected but noteworthy result, especially because the predictions of C_2 and GRI-2.11 mechanisms are in good agreement for both the premixed and diffusion flames.

To examine this aspect, we also computed the partially premixed flame using the GRI-3.0 mechanism as well as a 12-step augmented reduced mechanism.[16] The 12-step mechanism has been reduced from the GRI-1.2 mechanism. Figure 7 presents a comparison of the partially premixed flame structure in terms of temperature profiles computed using the GRI-2.11, GRI-3.0, and 12-step mechanisms. For $\phi = 1.5$, the nonpremixed zone obtained with the GRI-3.0 mechanism is located slightly closer to the premixed zone compared to that obtained with the other two mechanisms. The overall differences between the predictions of these three mechanisms are negligible. Thus, an important conclusion from Figs. 4 and 7 is that the partially

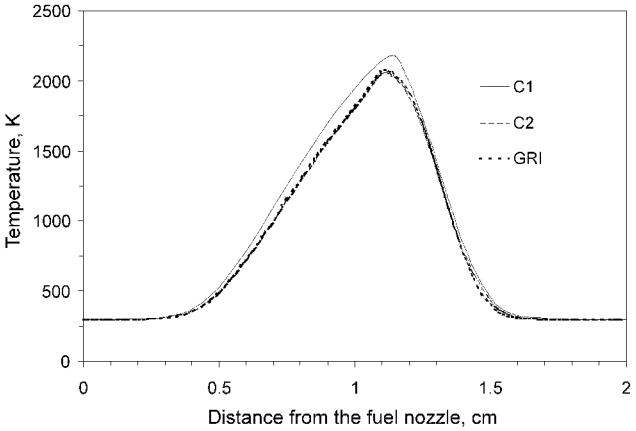

Fig. 6 Temperature profiles for a methane–air diffusion flame computed by using C_1, C_2, and GRI-2.11 mechanisms; fuel and air-stream velocities are 10 cm/s each; strain rate is 7.5 s^{-1}.

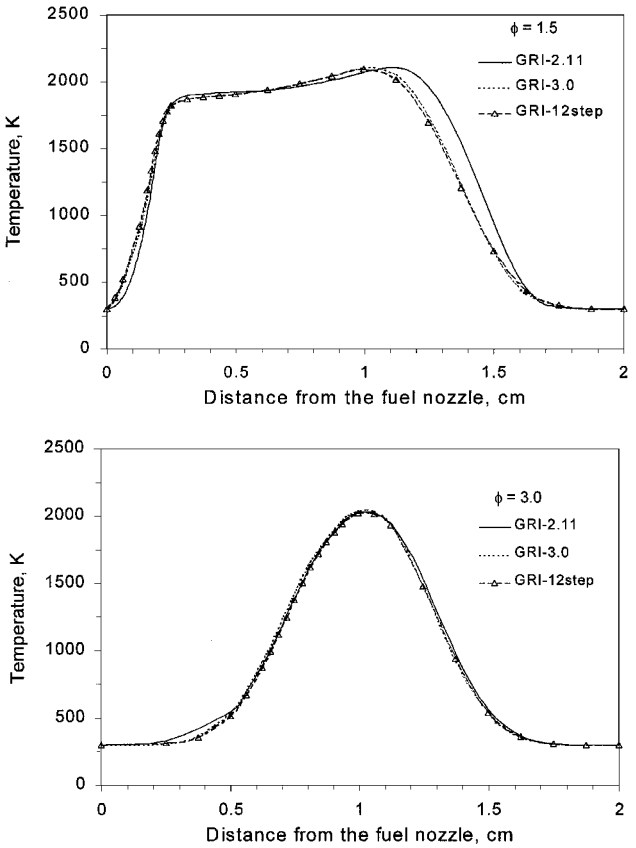

Fig. 7 Partially premixed flame structure in terms of temperature profiles obtained using the GRI-2.11, GRI-3.0, and 12-step reduced mechanisms corresponding to the conditions of Fig. 4.

premixed flame structure obtained using the C_1 and C_2 mechanisms is significantly different from that obtained using the GRI-2.11 and GRI-3.0 mechanisms. Measurements of the counterflow partially premixed flame structure at different levels of air premixing are needed to address these differences.

Differences Between C_1 and C_2 Mechanisms

There are notable differences between the predictions of C_1 and C_2 mechanisms. At higher level of air premixing, $\phi = 1.5$, the premixed reaction zone obtained using the C_2 mechanism is closer to the fuel nozzle than that using the C_1 mechanism. This implies that the methane consumption rate in the premixed reaction zone is higher for C_2 mechanism than that for C_1 mechanism. This is

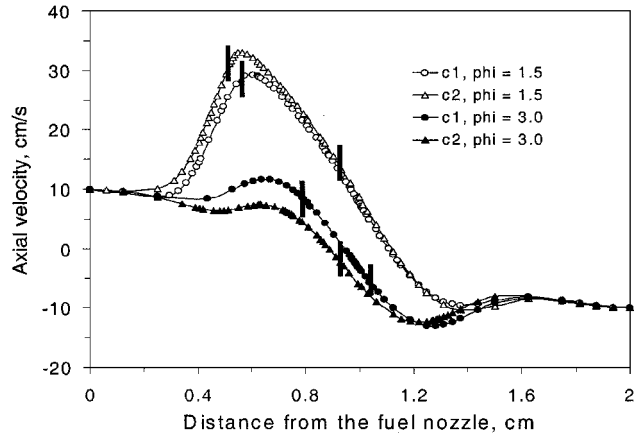

Fig. 8 Axial velocity profiles for the C_1 and C_2 mechanisms corresponding to the conditions of Fig. 4.

confirmed by the CH_4 consumption rate profiles that are presented later.

At lower level of air premixing, that is, $\phi = 3.0$, however, the situation is reversed. As indicated in Fig. 4b, the premixed reaction zone obtained using the C_1 mechanism is located closer to the fuel nozzle than that using the C_2 mechanism. These results are in accord with those reported by Shu et al.[18] for partially premixed flames in a planar configuration. As discussed in Ref. 18, the major effect of C_2 chemistry at lower equivalence ratios, $\phi = 1.5$, is to increase the overall reaction rates by increasing the H-atom formation and, thereby, augment the effect of chain-branching reactions by raising the availability of radical species. However, at higher equivalence ratios, $\phi = 3.0$, this effect is significantly diminished due to the paucity of O atoms, with the net result that the methane consumption rate is reduced when C_2 mechanism is employed. This is further confirmed by the H_2 mole fraction profiles shown in Fig. 5. For the C_2 mechanism, the H_2 mole fraction decreases significantly (note the peak value decreases from 0.04 to 0.017) as ϕ is increased from 1.5 to 3.0. The consumption of H_2 in the nonpremixed reaction zone occurs through the H_2–O_2 chemistry that also produces H and OH radicals. Consequently, a sharp reduction in the H_2 mole fraction implies a sharp decrease in the radical pool, and this is largely responsible for a much sharper decrease in the methane consumption rate for the C_2 and GRI-2.11 mechanisms compared to that for the C_1 mechanism, as ϕ is increased from 1.5 to 3.0.

The results shown in Figs. 4 and 5 also indicate that the premixed reaction zone obtained using the C_2 mechanism is more sensitive to the equivalence ratio compared with that using the C_1 mechanism. At $\phi = 1.5$, this zone for the C_2 mechanism is located closer to the fuel nozzle compared to that for the C_1 mechanism, whereas at $\phi = 3.0$, it is located farther from the fuel nozzle. Consequently, at higher level of air premixing, $\phi = 1.5$, the C_2 mechanism predicts a larger separation between the two reaction zones compared to the C_1 mechanism. However, at lower level of premixing, $\phi = 3.0$, the separation between the reaction zones is larger when the C_1 mechanism is used. In fact, the predictions with the C_2 mechanism indicate that the two reaction zones are beginning to merge at $\phi = 3.0$.

Figure 8 presents axial velocity profiles obtained using the C_1 and C_2 mechanisms. For $\phi = 1.5$, the lowest axial velocity in the near-exit region of the fuel jet, which can be regarded as the propagation velocity of the premixed flame, is higher for the C_2 mechanism than that for the C_1 mechanism. This is consistent with the results concerning the premixed flame speeds presented in Fig. 2. Note that the conventional premixed flame speed is not meaningful for $\phi \geq 1.5$ because these equivalence ratios are outside the rich flammability limit. However, the premixed flame speed is meaningful in the context of a partially premixed flame, in which the premixed reaction zone is stabilized due to synergistic interactions between the premixed and nonpremixed reaction zones. These interactions in a partially premixed zone extend the rich flammability limit of the premixed reaction zone.

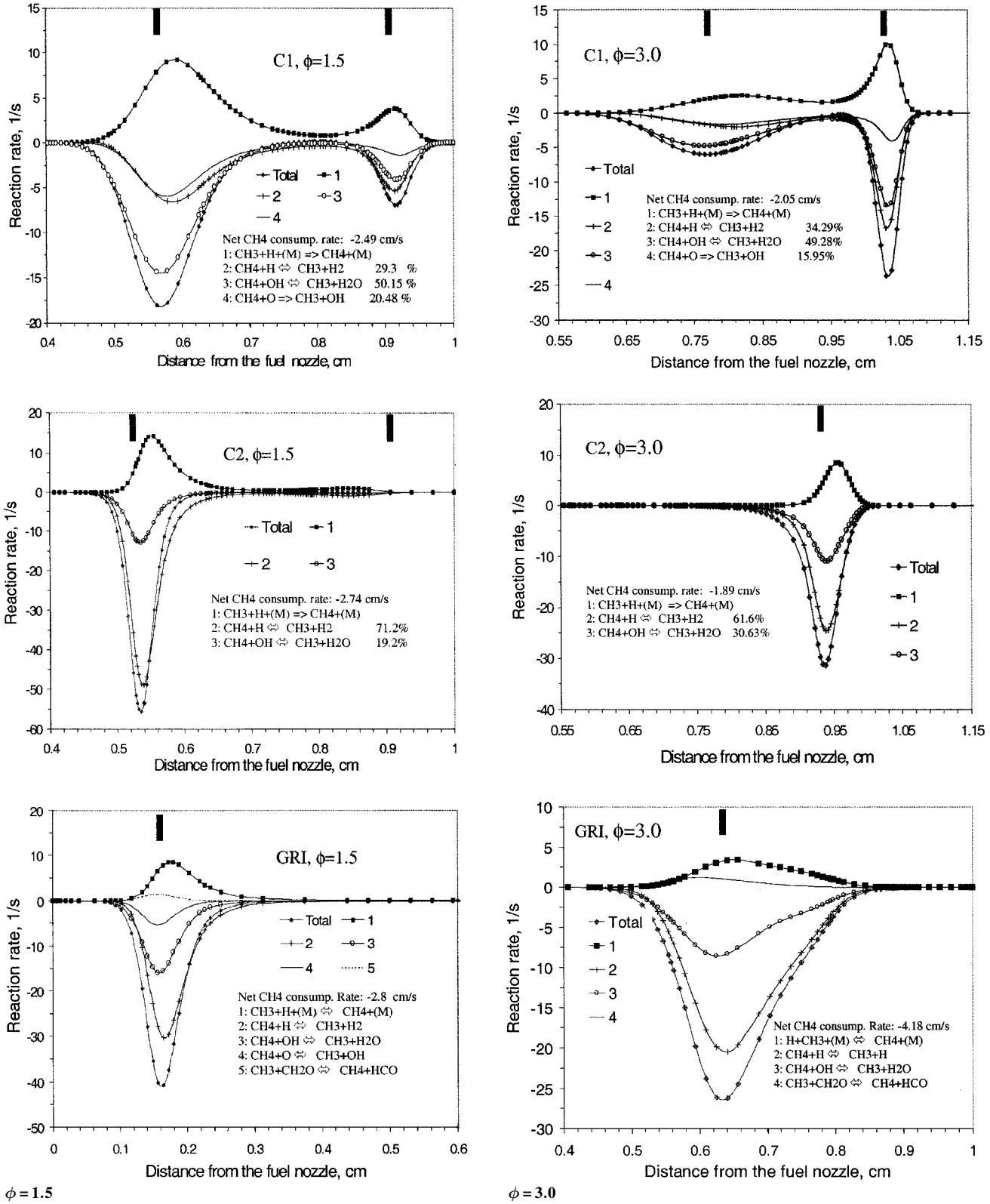

Fig. 9 CH_4 consumption rate profiles for C_1, C_2, and GRI-2.11 mechanisms for the conditions of Fig. 4, where, for each case, net consumption rate obtained by integrating the local consumption rate along the axial direction is also provided.

At $\phi = 3.0$, the premixed propagation velocity for the C_1 mechanism is higher than that for the C_2 mechanism. In addition, for the C_2 mechanism, the stretch rate experienced by the premixed reaction zone at $\phi = 1.5$ and 3.0 is, respectively, higher and lower compared to that for the C_1 mechanism. The differences between the C_1 and C_2 mechanisms as ϕ is varied from 1.5 to 3.0 imply that certain reactions in these mechanisms are sensitive to the changes in equivalence ratio. This aspect is discussed in the next section.

Comparison of Reaction Rate Profiles

In Fig. 9, we plot the methane consumption rate profiles for the C_1, C_2, and GRI-2.11 mechanisms. At a higher level of air premixing, $\phi = 1.5$, the total methane consumption rate profile for the C_1 mechanism contains two peaks corresponding to the premixed and nonpremixed reaction zones. In contrast, the profiles for the C_2 and GRI-2.11 mechanisms show only one peak corresponding to the premixed zone. In addition, the methane consumption rate in

the premixed zone for these two mechanisms is significantly higher than that for the C_1 mechanism. Consequently, for both the C_2 and GRI-2.11 mechanisms, methane is completely consumed in the premixed region with very little CH_4 escaping into the nonpremixed region. In contrast, when the C_1 mechanism is employed, a significant amount of methane leaks through the premixed zone, and the amount of leakage increases with ϕ. This is consistent with the CH_4 mass fraction profiles presented in Fig. 5. The higher fuel consumption in the premixed reaction zone for the C_2 and GRI-2.11 mechanisms is attributable to the C_2 chemistry, which provides an additional pathway for methyl consumption through the reaction $CH_3 + CH_3 \Leftrightarrow C_2H_6$.

As noted earlier, the premixed reaction zone for the GRI-2.11 mechanism is located very close to the fuel nozzle. The total methane consumption rate profiles for $\phi = 1.5$ corroborate this observation. For this mechanism, the peak value of the methane consumption rate occurs at a distance of 0.17 cm from the fuel nozzle, whereas those for the C_1 and C_2 mechanisms occur at 0.57 and 0.52 cm, respectively.

At the lower level of air premixing, $\phi = 3.0$, the two reaction zones are nearly merged when the C_2 and GRI-2.11 mechanisms are employed, whereas a double-flame structure is still observed when the C_1 mechanism is used. Another difference between the C_1 mechanism and the other two pertains to the dominant methane consumption reaction in the premixed reaction zone. For both the C_2 and GRI-2.11 mechanisms, methane consumption by H atoms dominates that by OH radicals, whereas for the C_1 mechanism, methane consumption by hydroxyl radicals is more important. This is again attributable to the C_2 chemistry that contributes to the higher concentration of H atoms for the C_2 and GRI-2.11 mechanisms compared with that predicted by the C_1 mechanism.

The profiles of total production rates of CO_2 and H_2O (not presented) indicated that at high level of air premixing, $\phi = 1.5$, the production of CO_2 and H_2O occurs mostly in the premixed zone when the C_2 mechanism is employed, whereas for the C_1 mechanism, the production of CO_2 and H_2O occurs in both the premixed and nonpremixed zones. This difference is because the methane consumption rate in the premixed reaction zone is much higher for the C_2 mechanism that for the C_1 mechanism. As a consequence, the heat release rate in the premixed zone is much higher for the C_2 mechanism than that for the C_1 mechanism, as shown in Fig. 10.

As indicated in Figs. 9 and 10, at $\phi = 3.0$, the two reaction zones are nearly merged when the C_2 mechanism is employed, whereas a double-flame structure still exists when the C_1 mechanism is used. The implication is that, compared to the C_1 mechanism, the two reaction zones merge at a lower equivalence ratio when either the C_2 or GRI-2.112 mechanism is used. Figures 9 and 10 also show that, for both the C_1 and C_2 mechanisms, the premixed zone chemistry is relatively more dominant at higher levels of air premixing, that is, lower ϕ, whereas the nonpremixed zone chemistry becomes more dominant at lower level of air premixing, that is, higher ϕ.

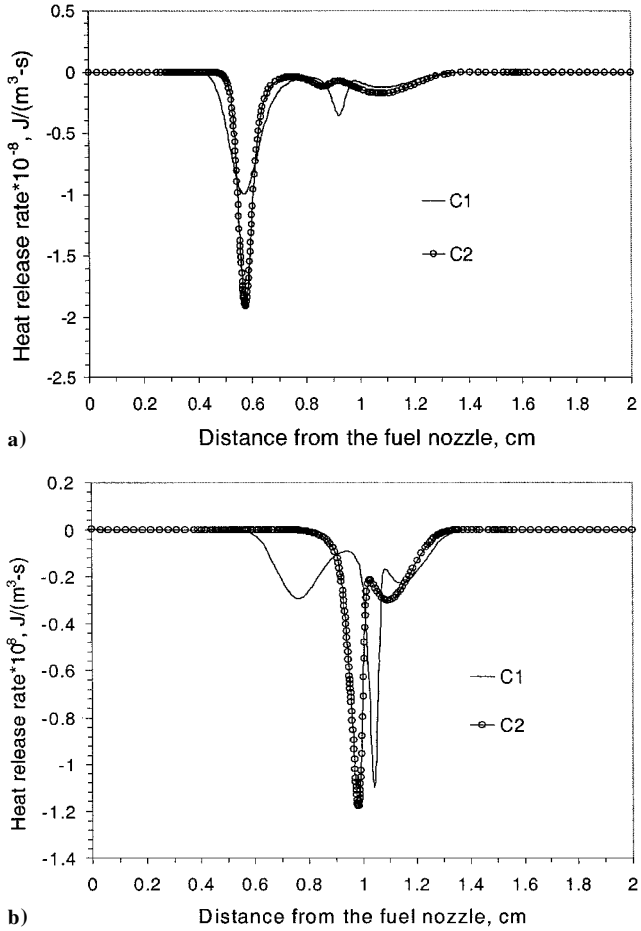

Fig. 10 Heat release rate profiles for the C_1 and C_2 mechanisms for the conditions of Fig. 4 at a) $\phi = 1.5$ and b) $\phi = 3.0$.

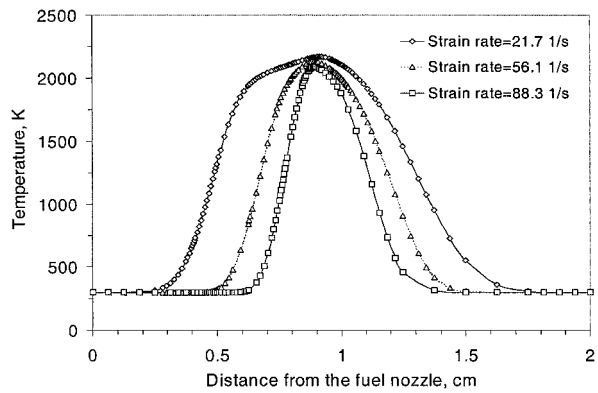

Fig. 11 Temperature profiles predicted by using the C_2 mechanism for three different strain rates at $\phi = 1.5$.

Effect of Strain Rate on Flame Structure

Figure 11 shows the flame structure, computed by using the C_2 mechanism, in terms of temperature profiles for three different strain rates at $\phi = 1.5$. The strain rate is increased by increasing the exit velocity of both the jets. As stated earlier, the strain rate is defined as the maximum value of the oxidizer-side velocity gradient just before the flame.[9] The strain rates of 21.7, 56.1, and 88.3 s^{-1} were obtained by increasing the jet exit velocities to 20, 40, and 60 cm/s, respectively. As shown in Fig. 11, the separation between the two reaction zones decreases as the strain rate is increased. As noted earlier, the reaction zones also tend to merge as the level of air premixing decreases, that is, ϕ increases from 1.5 to 3.0. There are, however, differences in the change of the partially flame structure caused by increasing the equivalence ratio compared to those caused by increasing the strain rate.

A comparison of Figs. 11 and 4 indicates that the temperature gradient on the fuel side increases as a_s is increased, whereas it decreases as ϕ is increased. The gradients of major species mole fractions follow a similar behavior. The changes in the gradients of temperature and species mole fractions can be attributed to a balance between convection, diffusion, and reaction. Increasing the equivalence ratio in the fuel stream directly affects the premixed zone chemistry, which then decreases the physical separation between the premixed and nonpremixed reaction zones. In contrast, increasing the strain rate changes the physical separation between two reaction zones without causing any changes in the reaction chemistry. As the two reaction zones get closer, the heat and radical transport between them is enhanced, which then changes the reaction chemistry of the premixed reaction zone. Thus, the partially premixed flame structure is relatively more sensitive to the equivalence ratio than the strain rate. More specifically, the equivalence ratio affects the structure of the partially premixed flame in the context of changing the premixed flame speed, whereas the strain rate affects reaction chemistry by changing the flame structure aerodynamically.

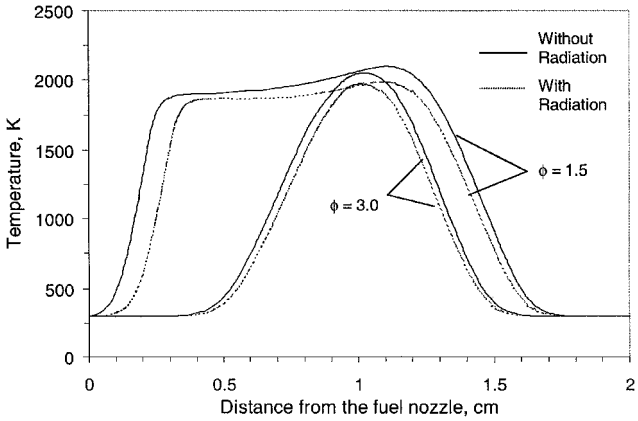

Fig. 12 Temperature profiles for partially premixed flames with and without radiation at $\phi = 1.5$ and 3.0.

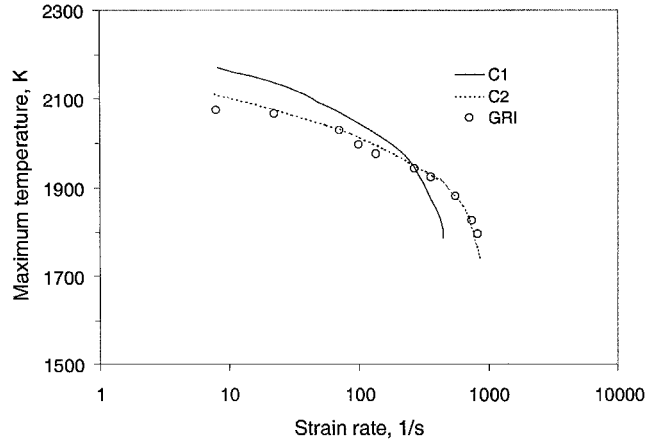

Fig. 13 The maximum flame temperature vs strain rate for the C_1, C_2, and GRI-2.11 mechanisms at $\phi = 1.5$.

Effect of Radiation Heat Transfer on Flame Structure

The effects of thermal radiation on methane–air partially premixed and diffusion flames have been studied by Zhu et al.[24] and Gore et al.[25] Their results showed that radiative heat loss caused by emission from gas molecules changes the temperature and NO mole fraction in low equivalence ratio partially premixed flames significantly. We have employed an optically thin model to examine the effect of radiation heat transfer on the partially premixed flame structure. The Oppdif code was modified to include the volumetric rate of radiation heat loss q_r in the energy equation. Following Ju et al.,[26] q_r can be written as

$$q_r = -4\sigma K_p\left(T^4 - T_\infty^4\right) \tag{1}$$

$$K_p = P_{CO_2}K_{CO_2} + P_{H_2O}K_{H_2O} + P_{CO}K_{CO} + P_{CH_4}K_{CH_4} \tag{2}$$

where σ is the Stefan–Boltzmann constant and T and T_∞ are the local and ambient temperatures, respectively. K_p is the Planck mean absorption coefficient of the mixture, and P_i and K_i are the partial pressure and Planck mean absorption coefficient of species i, respectively. The values for K_i are temperature dependent and are interpolated from Table 1 of Ju et al.[27]

Figure 12 presents a comparison of temperature profiles for flames, computed using the GRI-2.11 mechanism, with and without radiation at $\phi = 1.5$ and 3.0. The flame structure is not affected significantly, except that the temperature in the two reaction zones is reduced due to the radiation effect. In addition, with the radiation included, the premixed zone moves closer to the nonpremixed zone, although location of the nonpremixed zone is not affected by radiation. A comparison of the major species mole fraction profiles indicated a similar effect of radiation.

Effect of Reaction Mechanisms on Flame Extinction

A partially premixed flame will extinguish as the strain rate is increased above a critical value. In Fig. 13, we plot the peak temperature of partially premixed flame vs the strain rate at $\phi = 1.5$ for the C_1, C_2, and GRI-2.11 mechanisms. For low to moderate strain rates, the maximum temperature obtained using the GRI-2.11 mechanism is lower than that using the C_2 mechanism, which in turn is lower than that using the C_1 mechanism. The lower values for the GRI-2.11 mechanism are due to the heat loss to the burner because the premixed reaction zone with this mechanism is located very close to the fuel nozzle. The lower maximum temperature for C_2 mechanism compared to that for C_1 mechanism is due to the endothermic reactions associated with C_2 chemistry. At high strain rates, however, the maximum temperature for C_1 mechanism is lower compared to those for the other two mechanisms. This is because the strain rate at extinction is lower for the C_1 mechanism.

The critical strain rates near extinction obtained by using the C_1, C_2, and GRI-2.11 mechanisms are 450, 878, and 869 s^{-1}, respectively. The predicted extinction strain rate reported by Tanoff and Smooke[13] for a methane–air partially premixed flames at the same equivalence ratio is about 873 s^{-1}, which is close to the values obtained by using the C_2 and GRI-2.11 mechanisms. Chelliah et al.[9] investigated the extinction of methane–air diffusion flames employing the counterflow flame configuration, and reported an experimental extinction strain rate of 380 s^{-1}. Their predicted strain rate for extinction for the plug flow boundary conditions, which are also employed in this numerical study, was 391 s^{-1}. Thus, partially premixed flames are able to sustain significantly higher strain rates than the corresponding diffusion flames. The extinction flame temperature of the partially premixed flame obtained using the C_2 mechanism is 1740 K, which is slightly lower than the predicted value of 1758 K for the diffusion flame.[9]

Conclusions

The structure and extinction behavior of counterflow partially premixed flames have been investigated using five different chemistry models. The chemistry models include the C_1 and C_2 mechanisms of Peters and Rogg,[5] the GRI-2.11 mechanism, a 12-step augmented reduced mechanism, and GRI-3.0 mechanism. Simulations have focused on the comparison of these mechanisms in predicting the structure and extinction behavior of methane–air partially premixed flames over a wide range of strain rates and equivalence ratios, including those corresponding to premixed and diffusion flames.

Premixed flame speeds calculated using the C_2 and GRI-2.11 mechanisms are in good agreement with the experimental data, whereas those obtained using the C_1 mechanism show significant differences at fuel-rich conditions. However, the flammability limits ($0.5 < \phi < 1.4$) for methane–air mixtures obtained using these three mechanisms are almost identical. In addition, the diffusion flame structures computed using these mechanisms are essentially the same, except for small differences in the peak temperature values.

Results pertaining to partially premixed flames indicate all five mechanisms reproduce qualitatively the double-flame structure associated with these flames. There are, however, significant quantitative differences in the flame structures obtained using the C_1, C_2, and GRI-2.11 mechanisms. For low to moderate strain rates and high to moderate levels of air premixing, the GRI-2.11 mechanism yields a flame structure that is markedly different from that obtained using the other two mechanisms. For example, for a partially premixed flame established at $\phi = 1.5$ and a strain rate of 7.5 s^{-1}, the rich premixed reaction zone for the GRI-2.11 mechanisms is located very close to the fuel nozzle, which causes significant heat loss to the nozzle. In addition, the global flame for this mechanism is significantly broader compared to those for the other two mechanisms. This is somewhat unexpected but noteworthy result, especially because the predictions of C_2 and GRI-2.11 mechanisms are in good agreement for both the premixed and diffusion flames. Experimental data are needed to resolve these differences.

There are important quantitative differences in the structures of partially premixed flames simulated using the C_1 and C_2 mechanisms. First, the methane consumption rate in the premixed reaction zone is higher for the C_2 mechanism compared to that for the C_1 mechanism. Consequently, the formation rates of CO_2 and H_2O, as

well as the heat release rate in the premixed zone, are also higher for the C_2 mechanism. This is directly attributable to the C_2 chemistry, which provides an additional pathway for methyl consumption through the reaction $CH_3 + CH_3 \Leftrightarrow C_2H_6$. Second, the partially premixed flame structure obtained using the C_2-mechanism exhibits stronger sensitivity to the equivalence ratio compared with that using the C_1 mechanism.

As the equivalence ratio ϕ and/or the strain rate a_s are increased, the two reaction zones move closer and eventually merge into a single zone. The predicted values of ϕ, at which the merging occurs, is are smaller for the C_2 and GRI-2.11 mechanisms compared to that for the C_1 mechanism. For a given a_s, a further increase in ϕ yields a diffusion flame structure. On the other hand, a further increase in a_s (for a given ϕ) leads to flame extinction. The extinction strain rates obtained using the C_2 and GRI-2.11 mechanisms are significantly higher than that using the C_1 mechanism. For example, at $\phi = 1.5$, the extinction strain rates are 450, 878, and 869 s^{-1} for the C_1, C_2, and GRI-2.11 mechanisms, respectively.

An optically thin model has been used to examine the effect of radiation on the partially premixed flame structure. Results indicate that the flame structure is not affected significantly due to radiation, except that the temperature in the two reaction zones is reduced, and that the premixed zone is located slightly closer to the nonpremixed zone when the radiation is included.

Finally, the effect of an equivalent laminar flame speed on partially premixed flame structure has been examined. It is observed that the rich premixed zone has a propagation velocity that can be characterized in terms of an equivalent laminar flame speed corresponding to a given equivalence ratio. Because the velocity gradient on the fuel side is determined by the combined effects of this equivalent flame speed and the fuel jet exit velocity, the premixed flame speed plays an important role in determining the stretch rate and, therefore, the structure of partially premixed flames.

Acknowledgments

This research was partially supported by the National Science Foundation Combustion and Plasma Systems Program through Grant CTS-9707000 for which Farley Fisher is Program Director. Many fruitful and stimulating discussions with Ishwar K. Puri at the University of Illinois at Chicago are greatly appreciated.

References

[1]Yang, M. H., and Puri, I. K., "NO_x Formation in Stretched Premixed Flames Established Far from Extinction," *Fuel*, Vol. 72, No. 4, 1993, pp. 489–495.

[2]Williams, F. A., and Li, S. C., "Experimental and Numerical Studies of NO_x Formation in Two-Stage Methane–Air Flames," *Combustion and Flame*, Vol. 118, No. 3, 1999, pp. 399–412.

[3]Blevins, L. P., and Gore, J. P., "Computed Structure of Low Strain Rate Partially Premixed CH_4/Air Counterflow Flames: Implications for NO Formation," *Combustion and Flame*, Vol. 116, No. 4, 1999, pp. 546–566.

[4]Bowman, C. T., Hanson, R. K., Davidson, D. F., Gardiner, Jr., W. C., Lissianski, V., Smith, G. P., Golden, D. M., Frenklach, M., and Goldenberg, M., "GRI-MECH 2.11," URL: http//www.me.berkeley.edu/gri-mech/, 1995.

[5]Peters, N., and Rogg, B., *Reduced Kinetic Mechanisms for Applications in Combustion Systems*, Springer-Verlag, Berlin, 1993, pp. 8–12.

[6]Seshadri, K., and Peters, N., "Inner Structure of Methane-Air Flames," Combustion and Flame, Vol. 81, No. 2, 1990, pp. 96–118.

[7]Seshadri, K., "Multistep Asymptotic Analyses of Flame Structures," *Twenty-Sixth Symposium (International) on Combustion*, Combustion Inst., Pittsburgh, PA, 1996, pp. 831–846.

[8]Buipham, M., Seshadri, K., and Williams, F. A., "Asymptotic Structure of Premixed Methane–Air Flames With Slow CO Oxidation," *Combustion and Flame*, Vol. 89, No. 3–4, 1992, pp. 343–362.

[9]Chelliah, H. K., Law, C. K., Ueda, T., Smooke, M. D., and Williams, F. A., "A Experimental and Theoretical Investigation of the Dilution, Pressure and Flow-Field Effects on the Extinction Condition of Methane-Air-Nitrogen Diffusion Flames," *Twenty-Third Symposium (International) on Combustion*, Combustion Inst., Pittsburgh, PA, 1990, pp. 503–511.

[10]Yamaoka, I., and Tsuji, H., "The Structure of Rich Fuel-Air Flames in the Forward Stagnation Region of a Porous Cylinder," *Fifteenth Symposium (International) on Combustion*, Combustion Inst., Pittsburgh, PA, 1975, pp. 637–644.

[11]Yamaoka, I., and Tsuji, H., "Structure Analysis of Rich Fuel-Air in the Forward Stagnation Region of a Porous Cylinder," *Sixteenth Symposium (International) on Combustion*, Combustion Inst., Pittsburgh, PA, 1977, pp. 1145–1154.

[12]Yamaoka, I., and Tsuji, H., "An Experimental Study of Flammability Limits Using Counterflow Flames," *Seventeenth Symposium (International) on Combustion*, Combustion Inst., Pittsburgh, PA, 1979, pp. 843–855.

[13]Tanoff, M. A., and Smooke, M. D., "The Sensitive Structure of Partially Premixed Methane-Air vs. Air Counterflow Flames," *Twenty-Sixth Symposium (International) on Combustion*, Combustion Inst., Pittsburgh, PA, 1996, pp. 1121–1128.

[14]Sun, C. J., Sung, C. J., Zhu, D. L., and Law, C. K., "Response of Counterflow Premixed and Diffusion Flames to Strain Rate Variations at Reduced and Elevated Pressures," *Twenty-Seventh Symposium (International) on Combustion*, Combustion Inst., Pittsburgh, PA, 1996, pp. 1111–1120.

[15]Smooke, M. D., Seshadri, K., and Puri, I. K., "The Structure and Extinction of Partially Premixed Flames Burning Methane in Air," *Twenty-Second Symposium (International) on Combustion*, Combustion Inst., Pittsburgh, PA, 1988, pp. 1555–1563.

[16]Sung, C. J., Law, C. K., and Chen, J.-Y., "An Augmented Reduced Mechanism for Methane Oxidation with Comprehensive Global Parametric Validation," *Twenty-Sixth Symposium (International) on Combustion*, Combustion Inst., Pittsburgh, PA, 1998, pp. 295–304.

[17]Shu, Z., Krass, B. J., Choi, C. W., Aggarwal, S. K., Katta, V. R., and Puri, I. K., "Investigation of the Flame Structure of a Steady Two-Dimensional Partially—Premixed Methane–Air Flame," *Twenty-Sixth Symposium (International) on Combustion*, Combustion Inst., Pittsburgh, PA, 1998, pp. 625–632.

[18]Shu, Z., Katta, V. R., Puri, I. K., and Aggarwal, S. K., "Effects of C_2 Chemistry on the Structure of Partially-Premixed Methane–Air Flames," *Combustion Science and Technology* (to be published), 2000.

[19]Katta, V. R., and Roquemore, W. M., "Simulation of Dynamic Methane Jet Diffusion Flames Using Finite Rate Chemistry Models," *AIAA Journal*, Vol. 36, No. 11, 1994, pp. 2044–2054.

[20]Lutz, A. E., Kee, R. J., Grcar, J. F., and Rupley, F. M., "Oppdif: A Fortran Program for Computing Opposed-Flow Diffusion Flames," Sandia Rept. 96-8243, 1997.

[21]Kee, R. J., Rupley, F. M., and Miller, J. A., "Chemkin: A Fortran Chemical Kinetics Package for the Analysis of Gas Phase Chemical Kinetics," Sandia Rept. 89-8009B, 1993.

[22]Kee, R. J., Grcar, J. F., Smooke, M. D., and Miller, J. A., "A Fortran Program for Modeling Steady Laminar One-Dimensional Premixed Flames," Sandia Labs., SAND-85-8240, 1993.

[23]Vagelopoulos, C. M., Egolfopoulos, F. N., and Law, C. K., "Further Considerations on the Determination of Laminar Flame Speeds with the Counterflow Twin-Flame Technique," *Twenty-Fifth Symposium (International) on Combustion*, Combustion Inst., Pittsburgh, PA, 1994, pp. 1341–1347.

[24]Zhu, X. L., Takeno, T., and Gore, J. P., "A Study of the Effects of Thermal Radiation on Methane/Air Counterflow Partially Premixed Flames by Using Detailed Chemical Kinetics," *Proceedings of the First Joint Meeting of the U.S. Sections of the Combustion Institute*, Washington, DC, 1999, pp. 761–764.

[25]Gore, J. P., Lim, J., Takeno, T., and Zhu, X. L., "A Study of the Effects of Thermal Radiation on the Structure of Methane/Air Counter-Flow Diffusion Flames Using Detailed Chemical Kinetics," *Proceedings of the 5th ASME/JSME Joint Thermal Engineering Conference (CD)* (Book of Abstracts), San Diego, CA, 1999, p. 50.

[26]Ju, Y., Guo, H., Maruta, K., and Liu, F., "On the Extinction Limit and Flammability Limit of Non-Adiabatic Stretched Methane-Air Premixed Flames," *Journal of Fluid Mechanics*, Vol. 342, 1997, pp. 315–334.

[27]Ju, Y., Guo, H., Liu, F., and Maruta, K., "Effects of the Lewis Number and Radiative Heat Loss on the Bifurcation and Extinction of CH4/O2-N2-He Flames," *Journal of Fluid Mechanics*, Vol. 379, 1999, pp. 165–190.

J. P. Gore
Associate Editor